Laser and Particle Beams

cambridge.org/lpb

A coaxial-output rolled strip pulse forming line based on multi-layer films

Jian-Cang Su, Rui Li, Jie Cheng, Bin-Xiong Yu*, Xi-Bo Zhang, Liang Zhao and Wen-Hua Huang

Science and Technology on High Power Microwave Laboratory, Northwest Institute of Nuclear Technology, Xi'an, Shaanxi 710024, China

Original Study

*Current address: Northwest Institute of Nuclear Technology, No. 28, Pingyu Lu, Baqiao Qu, Xi'an, Shaanxi 710024, People's Republic of China

Cite this article: Su J-C, Li R, Cheng J, Yu B-X, Zhang X-B, Zhao L, Huang W-H (2018). A coaxial-output rolled strip pulse forming line based on multi-layer films. *Laser and Particle Beams* **36**, 69–75. https://doi.org/10.1017/S026303461700091X

Received: 24 May 2017
Accepted: 10 December 2017

Key words:
Coaxial output; multi-layer films; pulse-forming line; rolled strip line

Author for correspondence:
Binxiong Yu, Science and Technology on High Power Microwave Laboratory, Northwest Institute of Nuclear Technology, Xi'an, Shaanxi 710024, China. E-mail: yubinxiong@nint.ac.cn

Abstract

A coaxial-output rolled strip pulse-forming line (RSPFL) with a dry structure is researched for the purpose of miniaturization and all-solid state of pulse-forming lines (PFL). The coaxial-output RSPFL consists of a coaxial-output electrode (COE) and a rolled strip line (RSL). The COE is characterized by quasi-coaxial structure, making the output pulse propagate along the axial direction with a small output inductance. The RSL is rolled on the COE, whose transmission characteristics are analyzed theoretically. It shows that the RSL can be regarded as a planar strip line when the rolling radius of the strip line is larger than 60 times of the thickness of the insulation dielectric layer of RSL. CST modeling was carried out to simulate the discharging characteristic of the coaxial-output RSPFL. It shows that the coaxial-output RSPFL can deliver a discharging pulse with a rise time <6 ns when the impedance of the RSL matches that of the COE, which confirms the theoretical analysis. A prototype of the coaxial-output RSPFL was developed. A 49-kV discharging pulse on a matched load was achieved when it was charged to 100 kV. The discharging waveform has a pulse width of 32 ns, with a rise time of 6 ns, which is consistent with the simulation waveform. An energy-storage density of 1.9 J/L was realized in the coaxial-output RSPFL. By the method of multi-stage connection in series, a much higher output voltage is convenient to be obtained.

Introduction

A pulse-forming line (PFL) is the key component of a pulsed power device to generate high-voltage pulses with a width ranging from ns to μs. According to the structure, the PFL can be divided into the coaxial PFL, the strip PFL, the spiral PFL, and so on. Miniaturization of the PFL is an important direction for the development and application of pulsed power technology. Different methods have been applied to minimize the size of the PFL, including the stacked Blumlein line (Coogan *et al.*, 1990; Davanloo *et al.*, 1998; Liu *et al.*, 2009), Marx technology (Zhang & Liu 2013), the transmission line transformer (Graneau 1990; Yu *et al.*, 2014), generator based on Tesla transformer and pulse forming network (Su *et al.*, 2009), and so on. Compared with a conventional single coaxial PFL, the charging voltage of a PFL using one of the aforementioned methods is decreased, making it possible to employ insulation material with high-energy density as the energy dielectric to minimize the size and weight of a PFL.

In recent years, great progress has been made in the manufacturing technology of insulated film. Polypropylene (PP) films with good frequency characteristics and high-energy density are widely used in pulse capacitor under electric field strength >200 kV/mm (Laihonen & Gäfvert 2007). So, it is feasible to use the PP films as energy dielectric in the plane-plate PFL or the strip PFL to miniaturize a PFL. A strip PFL has three foil electrodes including two low-voltage (LV) foil electrodes and a high-voltage (HV) electrode. The HV foil electrode is located between the two LV foil electrodes, which forms an electromagnetic field distribution similar to that of a coaxial PFL. Due to its weak magnetic leakage, it is feasible to roll the strip PFL without waveform distortion when forming a pulse. But, there are some problems as to this technology. On one hand, since a rolled strip pulse-forming line (RSPFL) has two LV electrodes, the connecting inductance is large when the strip line is connected to the discharging circuit. As a result, it will distort the output pulse waveform. On the other hand, in order to improve the output voltage of the RSPFL, liquid insulation such as transformer oil is employed as an assistant insulation dielectric of the RSPFL, which goes against the tendency of all-solid state. Some researchers have already paid attention to the RSPFL (Yang *et al.*, 2010; Li *et al.*, 2015). The RSPFLs mentioned in the references have the advantages of compactness, portability, and long pulse achievability. However, apart from dipping in transformer oil, these RSPFLs are connected with the discharging circuit through a point, which leads to a large circuit inductance and an insufficient current flow capacity. So, the output pulses have rise times slower than 10 ns, at the same time, overheating occurs at the connection point.

© Cambridge University Press 2018

CAMBRIDGE UNIVERSITY PRESS

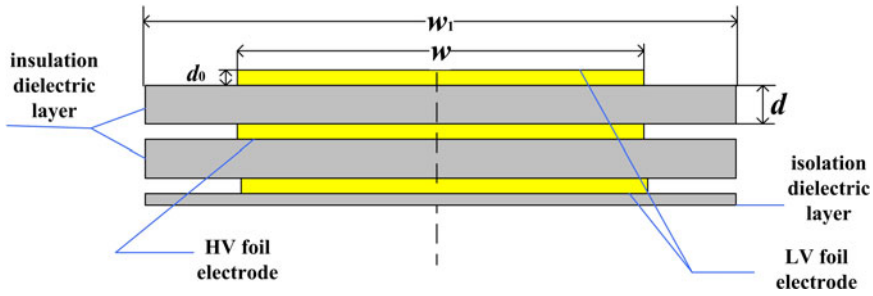


Fig. 1. Cross-sectional view of the strip line.

A coaxial-output RSPFL based on multi-layer films is developed in this paper. It has a small discharging inductance due to its coaxial-output structure. Instead of impregnation process, heat treatment is employed to eliminate the bubbles of edges of the foil electrodes, so that it has a dry structure. It is a feasible method for miniaturization and all-solid state of a PFL.

Principle of the coaxial-output RSPFL

Transmission characteristics of the rolled strip line (RSL)

The cross-sectional view of a strip line is shown in Figure 1. It contains three copper-foil electrodes, two insulation dielectric layers, and an isolation dielectric layer. The thicknesses of the three copper foils are d_0, and their widths are w. The thicknesses of the two insulation dielectric layers are both d. the width of two insulation dielectric layers and isolation dielectric layer are both w_1.

As shown in Figure 2, the strip line is rolled around the center axis with a rolling radius of R, and the rolled degree is $2\varphi_0$. Assume that a constant current, I_0, flows in HV foil electrode, and the current of $I_0/2$ flows in each of the two LV foil electrodes

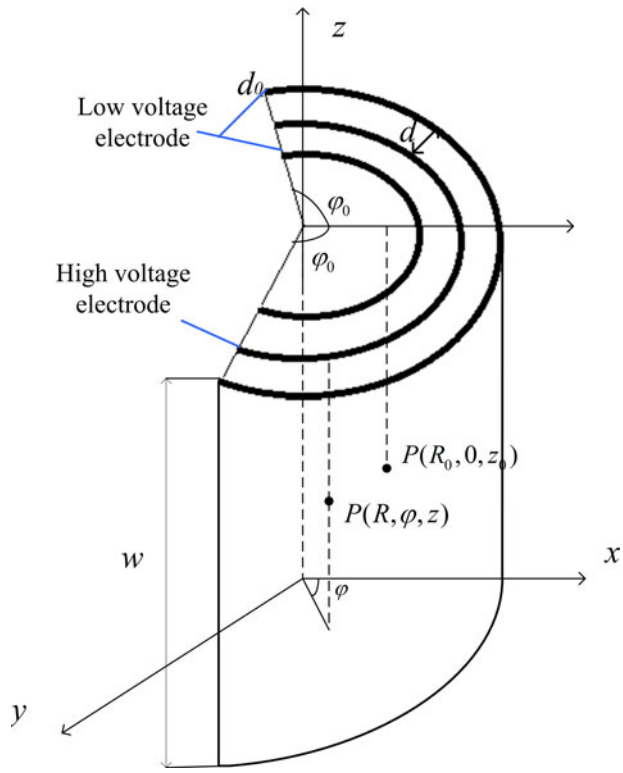


Fig. 2. Sketch of the RSL.

with opposite directions. According to the Faraday's law, the currents will induct a magnetic field. In a cylindrical coordinate system, the current density in the HV electrode at point $P_1(R, \varphi, z)$ is $jdzdl$, where $j = I_0/w$, and the magnetic flux density at point $P\ (R_0, 0, z_0)$ is

$$\begin{aligned} d\vec{B} &= \frac{\mu_0}{4\pi}\frac{jdzd\vec{l}\times\vec{r}}{r^3} \\ &= \frac{\mu_0 j}{4\pi}\frac{R[(z-z_0)\vec{e}_{r1}+(R-R_0\cos\varphi)\vec{e}_z]d\varphi dz}{((z-z_0)^2+R_0^2+R^2-2R_0aR\cos\varphi)^{3/2}}. \end{aligned} \tag{1}$$

Its axial component is derived as

$$dB_z = \frac{\mu_0 j}{4\pi}\frac{R(R-R_0\cos\varphi)}{(R_0^2-2R_0R\cos\varphi+R^2+(z_1-z_0)^2)^{3/2}}d\varphi dz. \tag{2}$$

So, the total axial magnetic flux density inducted by currents in the three foil electrodes is

$$B_{zt} = \frac{\mu_0 I}{4\pi w}\int_{-\varphi_0}^{\varphi_0}\left(f(R)-\frac{1}{2}f\left(R+\frac{d_0}{2}+d\right)-\frac{1}{2}f\left(R-\frac{d_0}{2}-d\right)d\varphi, \right. \tag{3}$$

where

$$\begin{aligned} f(x) = &\frac{x(x-R_0\cos\varphi)}{R_0^2-2R_0x\cos\varphi+x^2} \\ &\left[\frac{w-z_0}{\sqrt{R_0^2-2R_0x\cos\varphi+x^2+(w-z_0)^2}}\right. \\ &\left.+\frac{z_0}{\sqrt{R_0^2-2R_0x\cos\varphi+x^2+z_0^2}}\right] \end{aligned} \tag{4}$$

when R goes to infinite large, the RSL becomes a planar strip line whose maximum magnetic flux density is $\mu_0 I/2w$. When $w \gg d$, the leakage magnetic flux of the planar strip line is much small. In this condition, a planar strip line could generate ideal rectangular pulses. In order to analyze the variation law of the magnetic flux density versus the rolling radius R in the RSL, parameters of the RSL are set as $w = 20d$, $d_0 = 0$, and $z_0 = w/2$. The magnetic flux densities normalized by $\mu_0 I/2w$ against R/d are shown in Figure 3 for the case of a whole loop ($\varphi_0 = \pi$) and a part loop with a small degree ($\varphi_0 = 0.03\pi$), respectively.

Figure 3(a) shows the variation of magnetic flux density in the inner insulation dielectric layer ($R_0 = R-d/2$) and the outer insulation dielectric layer ($R_0 = R + d/2$) versus R/d when the strip line

https://doi.org/10.1017/S026303461700091X Published online by Cambridge University Press

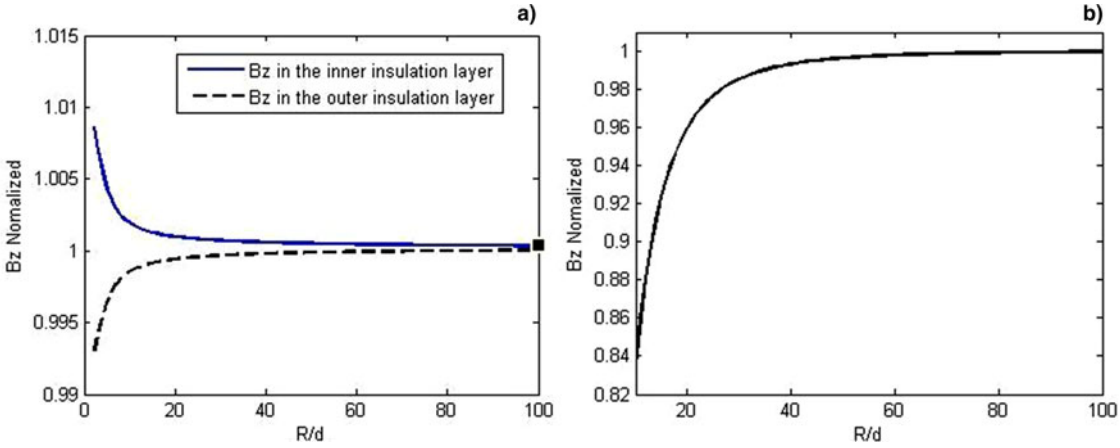


Fig. 3. Normalized magnetic flux density versus R/d in insulation dielectric of the RSL: (a) $\varphi_0 = \pi$; (b) $\varphi_0 = 0.03\pi$.

is rolled into a loop. From this figure, it is found that the two lines of magnetic flux density in the inner insulation dielectric and in the outer insulation dielectric get close to the value of $\mu_0 I/2w$ rapidly as R/d increases, which is the magnetic flux density in a planar strip line. Figure 3(b) shows the magnetic flux density in the outer insulation layer of the RSL when it is rolled with a small degree of 0.03 π. It shows that the magnetic flux density is gradually close to $\mu_0 I/2w$ when $R > 60d$, which illustrates that the magnetic flux density of the RSL is contributed by the current unit nearby if $R > 60d$. In this condition, the magnetic flux density will not be affected by the current in adjacent turns of the RSL. So, it is concluded that the RSL can be regarded as a planar strip line when $R > 60d$ with a characteristic impedance (Pozar, 2006).

$$Z_0 = \frac{60\pi d}{\sqrt{\varepsilon_r}(w + 0.882d)}, \quad w/2d > 0.35, \tag{5}$$

where ε_r is the relative permittivity of the insulation dielectric (PP films).

According to the principle of transmission line, the unit capacitance C_0 and the unit inductance L_0 of the RSL is

$$\begin{cases} C_0 = \dfrac{\sqrt{\varepsilon_r}}{cZ_0} = \dfrac{2\varepsilon_0\varepsilon_r(w + 0.882d)}{d}, \\ L_0 = \dfrac{Z_0\sqrt{\varepsilon_r}}{c} = \dfrac{\mu_0 d}{2(w + 0.882d)}. \end{cases} \tag{6}$$

The discharging pulse width τ is

$$\tau = \frac{2l\sqrt{\varepsilon_r}}{c}. \tag{7}$$

The copper-foil electrodes should be thicker than the depth of penetration to conduct large discharging current. The depth of penetration caused by the skin effect is

$$h = \sqrt{\frac{1}{\pi f \mu_0 \sigma}}, \tag{8}$$

where f is the average frequency of the discharging pulse; μ_0 is the permeability of vacuum; ε_0 is the permittivity of vacuum; c is the speed of light in vacuum; σ is the conductivity constant of copper; l is the length of the strip line.

Principle of coaxial output

A simplified sketch map of the coaxial-output RSPFL is shown in Figure 4. The simplified coaxial-output electrode (COE) can be considered as a short coaxial line, which contains an inner cylinder, an outer cylinder, and an insulation support. The RSL is rolled on the COE around the center axis. Starting ends of the two LV electrodes of RSL are connected to the outer cylinder, and the starting end of HV electrode of the strip line is connected to the inner cylinder through a hole in the outer cylinder. The coaxial-output structure is required to discharge along the axial direction at first, and the rise time of the discharging pulse is fast because the coaxial discharging inductance is small. Then, the pulse generated by the RSL is injected into the coaxial-output structure, and output along the axial direction. It is required that the characteristic impedance of the RSL equals to the circular impedance of the COE. So, the pulse generated by the RSL will reach each point of the circle of the coaxial-output structure without reflection. The circular impedance of the COE is approximately derived as

$$Z_1 = \frac{60\pi d_1}{\sqrt{\varepsilon_{r1}}S}, \tag{9}$$

where d_1 and ε_{r1} are the thickness and the relative permittivity of the insulation support, respectively. S is the effective width of a coaxial-output structure.

Development of coaxial-output RSPFL

Design of the RSL

A PFL with a characteristic impedance of 4.4 Ω is required in our laboratory to generate pulses with a pulse width of 30 ns, and its maximum charging voltage is 100 kV. The thickness of the insulation dielectric layer, d, is designed as 1 mm formed by 10-μm PP films of 100 layers. According to the test results, the breakdown voltage of PP films of 100 layers is as high as 200 kV. The relative permittivity of PP films, ε_r, is 2.2. It is derived that the width of three copper-foil electrode, w, is 28.4 mm according to Eq. (6).

https://doi.org/10.1017/S026303461700091X Published online by Cambridge University Press

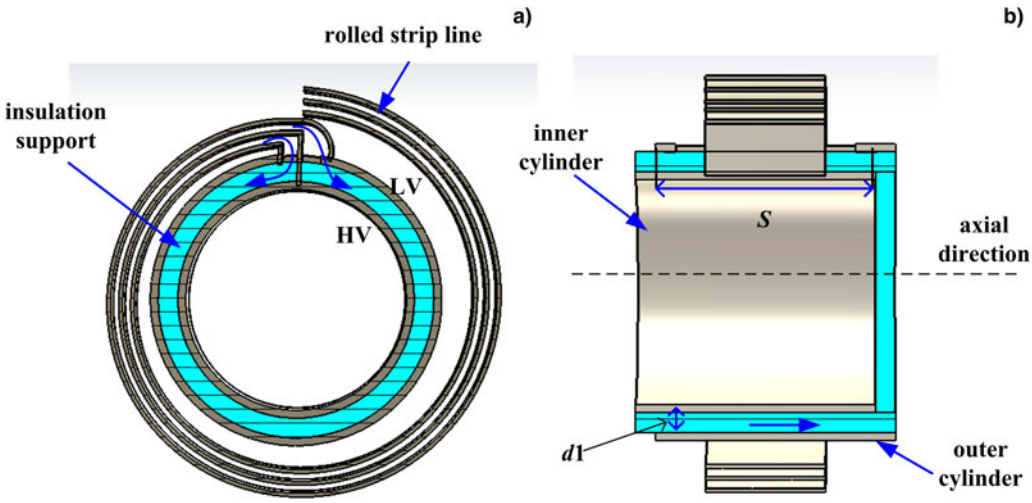


Fig. 4. A simplified sketch map of the coaxial-output RSPFL consisting of an RSL and a COE.

The average frequency of the discharging pulse with a width of 30 ns is about 30 MHz. According to Eq. (8), the depth of penetration in copper is calculated as 12 μm. The thickness of the electrodes, d_0, should be larger than 12 μm. Actually, copper foils with a thickness of 50 μm are used. The width of the insulation dielectric layer, w_1, is determined as 70 mm. The isolation dielectric layer is located between the two LV foil electrodes, and there is no potential difference in the isolation dielectric layer. So, the thickness of the isolation dielectric layer is determined as 0.2 mm, including 20 layers of 10-μm PP films. The length of the strip line, l, is determined as 3 m to generate a pulse with a width of 30 ns according to Eq. (7).

Structure of the COE

The COE plays a role of coaxial output. Its structure is shown in Figure 5. It contains an inner metal electrode, an insulation support, an outer electrode with a cavity, a cover of the cavity, and a connective electrode. The inner metal electrode and the outer electrode could be considered as the inner and the outer cylinders of a coaxial line, respectively. The insulation support is located between the inner and the outer electrodes, and it is made of polyimide material. It could endure the voltage between the inner and the outer electrodes. There is a rectangular hole in the outer electrode. The connection electrode, which is electrically connected with the inner electrode, is located in the middle of the rectangular hole. In the middle of the connection electrode, there is a perforating strip hole, through which the starting end of the HV foil of the strip line connects to the inner electrode. The area where the rectangular hole is located should be carefully treated to make sure the surface is smooth.

R_a is the smallest rolling radius of the RSL, and it is 120 mm, which is larger than 60 times of the width of the insulation dielectric layer. The outer diameter of the COE, D_0, is 284 mm, and its

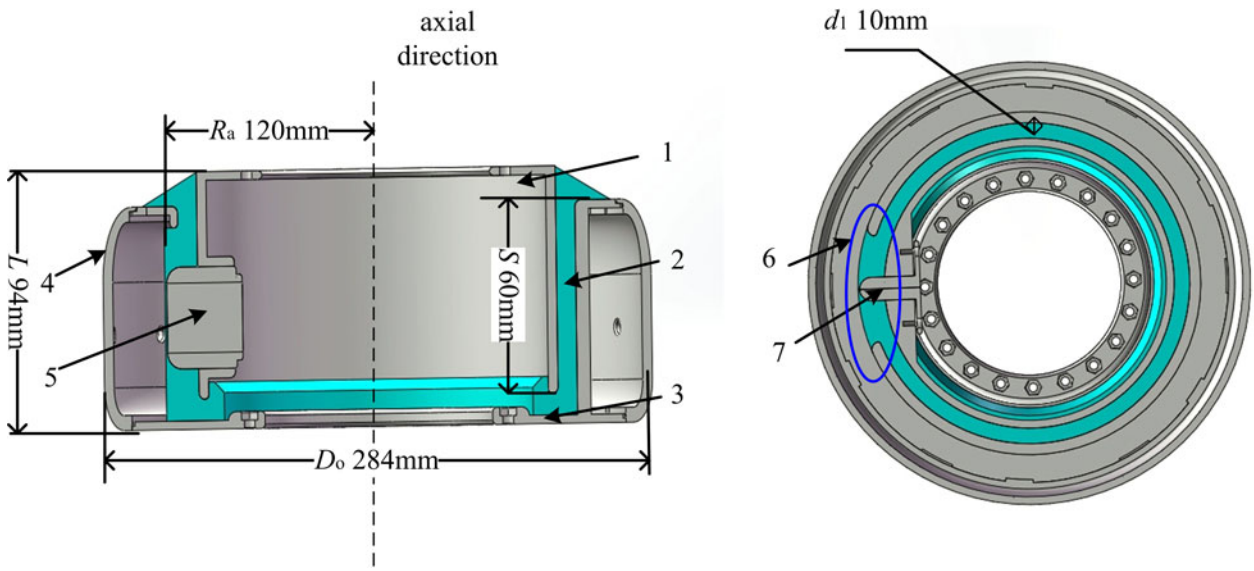


Fig. 5. Stretch of the COE:1, inner electrode; 2, insulation support; 3, outer electrode; 4, cover of the cavity; 5, connective electrode; 6, rectangular hole; 7, perforating strip hole.

https://doi.org/10.1017/S026303461700091X Published online by Cambridge University Press

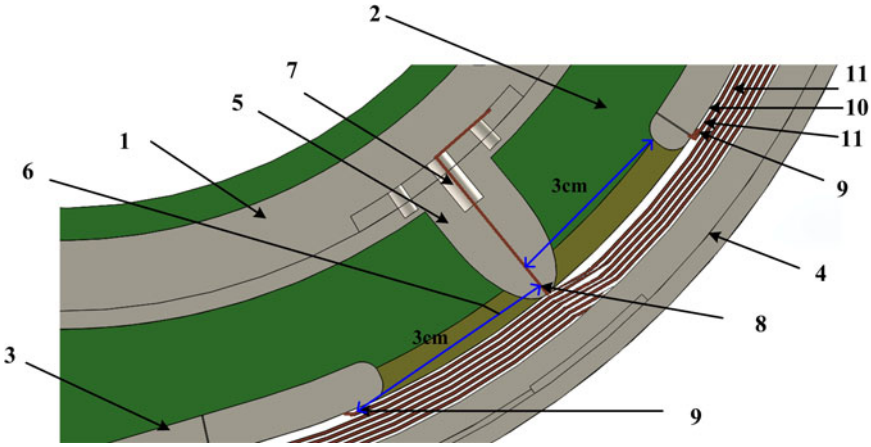


Fig. 6. Sketch of connection between the COE and RSL: 1, inner electrode; 2, insulation support; 3, outer electrode; 4, cover of the cavity; 5, connecting electrode; 6, rectangular hole; 7, perforating strip hole; 8, HV foil electrode; 9, LV foil electrode; 10, isolation insulation layer; 11, insulation dielectric layer.

maximum length, L, is 94 mm. The effective width of the COE, S, is 60 mm. According to Eq. (9), the matched thickness of the insulation support is about 4 mm. However, the real thickness is determined as 10 mm in order to endure the charging voltage of 100 kV.

The total RSPFL

A rolling machine with multiple rolling axes is employed to roll the strip line. At the beginning, all the ends of films and foil electrodes are fixed on the COE. The distance between the starting end of the HV foil and the starting ends of the two LV foils are both 3 cm in order to reduce the connection inductance between the RSL and the COE. Starting ends of 100 layers of PP films forming the insulation dielectric layer are uniformly distributed in a distance of 3 cm, so as to reduce air gap in the 3-cm area. After all ends of the strip line are well fixed, the strip line is rolled in the cavity of the outer electrode. Then, they are heated to 125°C for 3–5 h to eliminate the air bubbles beside the foil electrodes, by this means, discharging voltage along the surface will increase. At the same time, the developed RSPFL has a dry structure with a compression factor close to 1, which is convenient for the parameter design of the RSL (Fig. 6).

The picture of the COE is shown in Figure 7a, and the developed coaxial-output RSPFL without a cover is shown in Figure 7b.

Co-simulation of circuit and transient field

Modeling was done using CST Microwave Studio. A transient solver (Petrella, *et al.*, 2016) using a co-simulation of both ideal circuit elements and three-dimensional (3D) models was used to combine circuit models of the resistor and power supply with a physical model of the RSPFL. Figure 8 demonstrates this concept and shows the hybrid setup. The figure shows a voltage supply in series with the resistor (R_1), an inductor (L_1) and the RSPFL. Parameters of the RSPFL model are shown in Table 1, which are mostly the same as the theoretic design in the section "Development of coaxial-output RSPFL".

The real thickness of the foil electrodes, d_0, was 50 μm, which made the finite-element numbers in simulation too many to carry out. In order to lower the simulation difficulty, d_0 was set as 1 mm in the modeling. According to Cohn (1955), the edge capacitance of the foil electrodes would cause the characteristic impedance of the RSL a little smaller. This influence could be accurately calculated in the simulation. According to finite-element simulation, the characteristic impedances of planar strip lines with d_0 of 50 μm and 1 mm were calculated as 4.32 and 4.22 Ω, respectively.

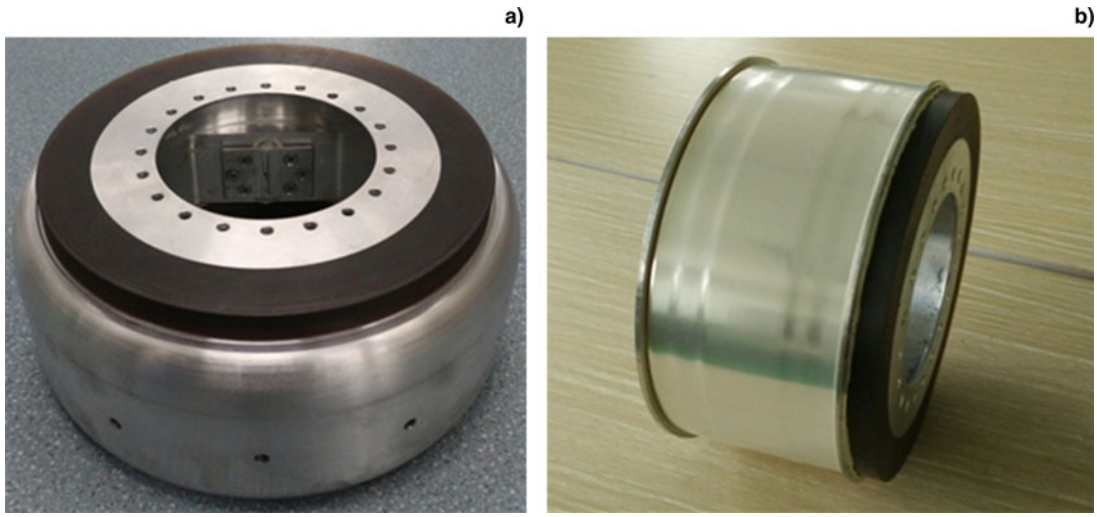


Fig. 7. Picture of the developed coaxial-output RSPFL: (a) The COE; (b) The RSPFL without the cover.

https://doi.org/10.1017/S026303461700091X Published online by Cambridge University Press

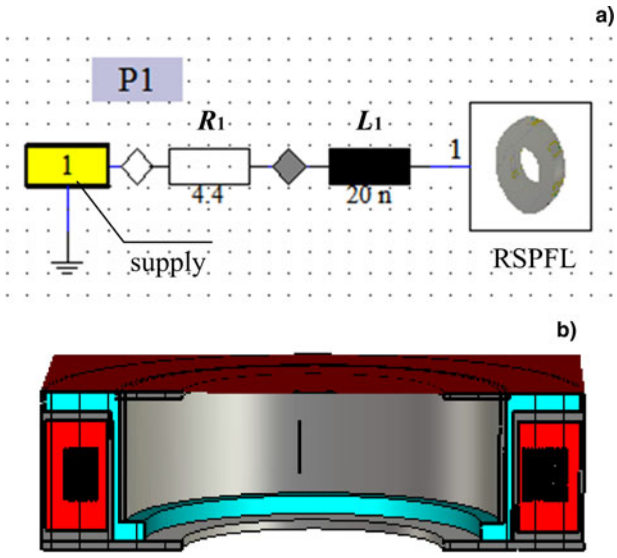


Fig. 8. The CST Microwave Studio co-simulation. (a) A combination of 3D modeling and discrete circuit elements. (b) A sectional view of the coaxial-output RSPFL model.

Table 1. Parameters of the RSPFL in the CST modeling compared with the design value

Parameters	Values in the modeling	Design value
w	28.4 mm	28.4 mm
d_0	1 mm	0.05 mm
w_1	70 mm	70 mm
d	1 mm	1 mm
l	2.8 m	2.8 m
d_1	4 and 10 mm	10 mm
R_a	100 mm	120 mm

Besides, as the volume of the RSL became larger, the smallest rolling radius of the RSL (R_a) was decreased to 100 mm in the modeling. However, R_a was still larger than 60 d.

An equivalent circuit of the discharging progress is simulated. The voltage supply is a step signal with an amplitude of 1 V, and L_1 and R_1 are set as 20 nH and 4.4 Ω, respectively. There is a probe (P_1) to record the voltage differential V_0 on R_1, whose theoretic amplitude is $R_1/(R_1 + Z_0)$. The pulse waveform of V_0 is the same as the discharging waveform of the RSPFL on R_1.

The simulations were carried out when the thickness of the insulation support (d_1) was set as 4 and 10 mm, respectively. The simulation result was shown in Figure 9. From the figure, it was found that the voltage pulse on R_1 has a pulse width of 33 ns, with amplitude of 0.51 V. So, the simulation impedance of the RSL, Z_0, was calculated as $Z_0 = (1–0.51)/0.51 \times 4.4 = 4.227$ Ω, which was the same as the impedance of a planar strip line with the same cross-section. It shows that the RSL can be regarded as a planar strip line when the rolling radius of the strip line is larger than 60d. As the simulation impedance of the strip line with d_0 of 50 μm was 4.32 Ω, while the theoretic value was 4.4 Ω. the relative error was 2.8%, which was acceptable for an engineering design.

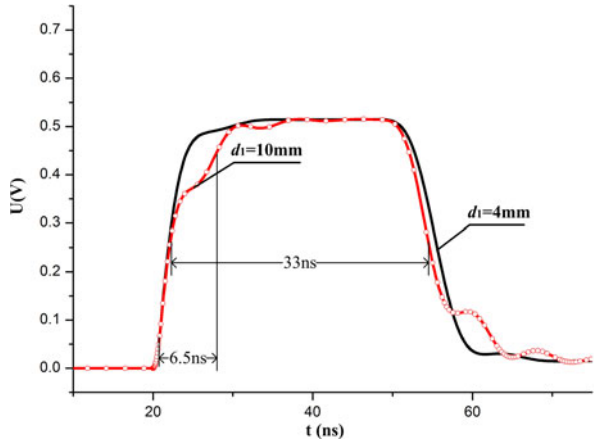


Fig. 9. Simulation equivalent discharging pulse waveform of the RSPFL.

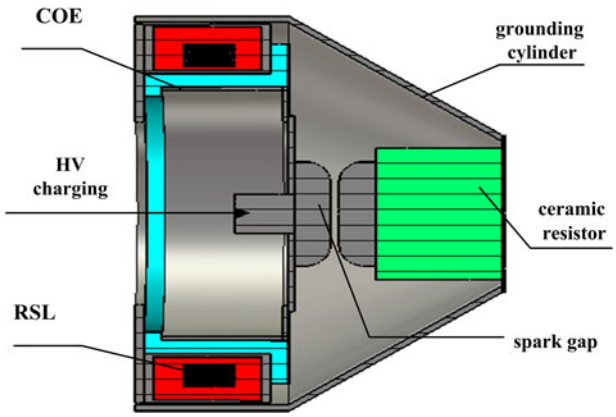


Fig. 10. Structure sketch of the testing circuit of the RSPFL.

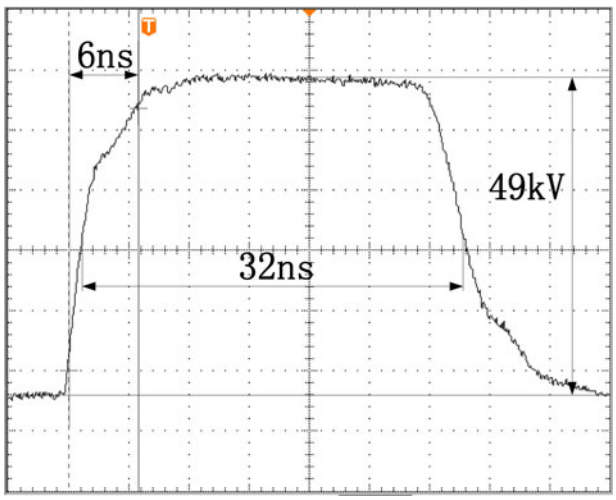


Fig. 11. Output pulse waveform of the RSPFL on a 4.4-Ω load.

There was a reflection in the rise time of the output pulse when d_1 was 10 mm, and the reflection was much smaller when d_1 became 4 mm. As the analysis in the subsection "Structure of the COE", the reflection occurred because the impedance of the RSL did not match the impedance of the COE when $d_1 = 10$ mm. The pulse width of the pulse is 33 ns, which was larger than the theoretic design as the COE was contributed to the pulse width, which generated the additional three nanoseconds.

https://doi.org/10.1017/S026303461700091X Published online by Cambridge University Press

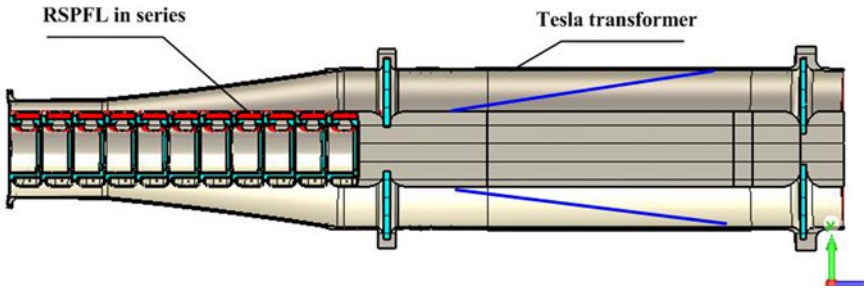


Fig. 12. Structure of a Tesla-style pulse generator based on RSPFL in series.

Experiments and results

The capacitance of the developed RSPFL, which contains the capacitance of the COE and the capacitance of the RSL, was measured as 3.54 nF by an RLC meter. The capacitance of the COE was measured as 140 pF. So, the capacitance of the RSL was 3.4 nF, while the value calculated by Eq. (7) was 3.41 nF. The relative error was smaller than 1%.

Voltage endurance capability of the developed RSPFL was tested in a high-pressure atmosphere as the structure sketch shown in Figure 10. A DC supply was applied to charge the RSPFL. When the RSPFL was charged to 100 kV, the spark gap located between the RSPFL and the load broke down. Then, a voltage pulse with an amplitude of 49 kV was generated on the 4.4-Ω ceramic resistor load. The output waveform is shown in Figure 11.

The amplitude of the discharging pulse is less than the theoretic amplitude on a matched load, which is 50 kV because of the loss in the spark gap. The discharging voltage pulse has a pulse width of 32 ns, with a pulse rise time as short as 6 ns and the amplitude fluctuation of the pulse flattop is <5%. Similar with the simulation waveform, there is a reflection in the rise time of the discharging pulse as d_1 is 10 mm in order to ensure the voltage endurance capability of the COE.

The maximum charging voltage of the developed coaxial-output RSPFL is 100 kV with a lifetime of less than pulses because breakdown along the surface, and the lifetime will increase to 10,000 pulses because of volume breakdown if the charging voltage decreases to 80 kV. The maximum energy density of the developed coaxial-output RSPFL is calculated as 1.9 J/L. the energy density of the RSPFL is much larger than that of transformer oil. However, the pulse lifetime is shorter than foiled capacitor impregnated in oil. There are two reasons: the first one, as the insulation thickness of the RSPFL is 1 mm, while that in the capacitor is usually smaller than 0.1 mm. So, the electric field enhance in RSPFL is much large than that in the capacitor if the even electric field is the same. The second one, the RSPFL with a dry structure is difficult in heat dissipation so that corona breakdown occurs.

The coaxial-output RSPFL is modularized, and it is convenient to realize multi-stage connection in series to acquire a much higher operating voltage (Graneau, 1990). As shown in Figure 12, The PFL of the generator based on Tesla transformer is formed by 11 stages of RSPFLs, which has a similar structure with the PFL shown in (Su *et al.*, 2009). The inner electrode of the front stage of RSPFL is connected to the outer electrode of the next stage, and the like. If the charging voltage of each RSPFL is 80 kV, then the charging voltage of PFL formed by 11 stages of RSPFLs will reach 800 kV. At the same time, the output waveform will be much better than that shown in (Su *et al.*, 2009), because the RSPFL has a coaxial-output structure, which will decrease the inductance of series loop. This work is under process.

Conclusions

A coaxial-output RSPFL based on stacked films has been proposed and developed in this paper. Three advantages of the RSPFL were achieved as follows. Firstly, its energy density reached as high as 1.9 J/L, which was much higher than that of a coaxial PFL using transformer oil as the insulation material. So, it is feasible to realize the miniaturization of the PFL. Secondly, it can deliver a discharging pulse with a rise time of 6 ns on a matched load, and the amplitude fluctuation of the pulse flattop was < 5%. Finally, modularization and miniaturization of the coaxial-output RSPFL are both realized, and it is convenient to obtain high output voltage through connecting multi-stage of modules in series. The pulse discharging test showed that the RSPFL can generate a 49-kV pulse with a pulse width of 32 ns on a matched load of 4.4 Ω. It is necessary to increase the lifetime of the RSPFL in future work before the RSPFL can be used in a repetitive frequency-operating generator.

References

Cohn SB (1955) Problems in strip transmission lines. *IRE Transactions on Microwave Theory and Techniques* **3**, 119–126.

Coogan JJ, Davanloo F and Collins CB (1990) Production of high-energy photons from flash x-ray sources powered by stacked Blumlien generators. *Review of Scientific Instruments* **61**, 1448.

Davanloo F, Collins CB and Agee J (1998) High-power, repetitive-stacked Blumlein pulsers commutated by single switching element. *IEEE Transactions on Plasma Science* **26**, 1463–4751.

Graneau PN (1990) The operation and modeling of transmission line transformers using a referral method. *Review of Scientific Instruments* **70**, 3180.

Laihonen SJ and Gäfvert U (2007) DC Breakdown strengths of polypropylene films: area dependence and statistical behavior. *IEEE Transactions on Electrical Insulation* **14**, 275–286.

Li S, Gao JM, Yang HW and Qian BL (2015) A high-voltage, long-pulse generator base on magnetic pulse compressor and Blumlein-type rolled strip pulse forming line. *Laser and Particle Beams* **33**, 511–518.

Liu JL, Cheng XB and Qian BL (2009) Study on strip spiral Blumlein line for the pulsed forming line of intense electron-beam accelerators. *Laser and Particle Beams* **27**, 95–102.

Petrella RA, Xiao S and Katsuki S (2016) An air core pulse transformer with a linearly integrated primary capacitor bank to achieve ultrafast charging IEEE transa. *Electrical Insulation* **23**, 2443–2449.

Pozar DM (2006) *Microwave Engineering*. Hoboben: Wiley.

Su JC, Zhang XB and Liu G.Zh. (2009) Long-pulse electron beam generator based on Tesla transformer and pulse forming network. *IEEE Transactions on Plasma Science* **37**, 1954–1958.

Yang S, Zhong HH, Qian BL and Yang HW (2010) An all-solid state, rolled strip pulse forming line with low impedance and compact structure. *Review of Scientific Instruments* **81**, 043303.

Yu B, Su JC and Li R (2014) A novel structure of transmission line pulse transformer with mutually coupled windings. *Review of Scientific Instruments* **85**, 035110.

Zhang Y and Liu JL (2013) A new kind of solid-state Marx generator based on transformer type magnetic switches. *Laser and Particle Beams* **31**, 239–248.

https://doi.org/10.1017/S026303461700091X Published online by Cambridge University Press